SPACE DEBRIS SEARCH AND TRACK FORWARD SCATTER RADAR SYSTEM WITH DIFFERENT PHASED ARRAY ANTENNAS

Sebastián Díaz Riofrío[1], Carmine Clemente[1], Christos Ilioudis[1], Massimiliano Vasile[1], and Nobuyuki Kaya[2]

[1] *University of Strathclyde, Glasgow, United Kingdom, Email: {sebastian.diaz-riofrio, carmine.clemente, c.ilioudis, massimiliano.vasile}@strath.ac.uk*

[2] *WaveArrays, Inc, Japan, Kobe University, Japan. Email: n.kaya@wavearrays.com*

ABSTRACT

Each day there are more space objects flying over the Earth resulting in a need to track and catalogue these objects, especially if they are non-cooperative, such as space debris. A good option for the detection of space debris are radar systems. However, with an overcrowded frequency spectrum a passive choice is more desirable. Thanks to the research being done in forward scatter and CubeSat systems, this seem good options to be examined. In view of the system to be fitted into a CubeSat and the antenna being one of the most delimiting aspects in this area, it is worth examining different antenna types to find the optimal antenna for the analysed scenario.

Keywords: radar; track; search; phased array; beam pattern; forward scatter; link budget; minimum detectable size, multiple integration.

1. INTRODUCTION

The increasing number of space objects orbiting around the Earth, from large satellites to small CubeSats, has created the need for systems that can detect and track space debris in order to have it localized and for the satellites not to collide with it. Certainly, there are on-the-ground systems using both radar and optical techniques that can detect and track space debris. However, these systems, such as FGAN's tracking and imaging radar (TIRA), are expensive and not accessible to every potential end user, academic or commercial. Moreover, many of the antennas used for space surveillance are primarily used in radio astronomy, so having a radar-only antenna would be more convenient and practical. Thus, a reliable, easily accessible and cheap, compared to the established systems, implementation would be useful.

In [1] it was described a system that consisted of a passive bi-static radar (PBR) deployed on a CubeSat, equipped with software defined radio (SDR), and an antenna so that the radar tasks for space surveillance could be performed. The paper showed that such a could be a low budget solution and could detect space debris of even a few centimetres. This will be a cheaper solution because, since the system will be positioned in a orbit, it will have shorter distances and smaller relative speeds, which will lead to easily achievable suitable signal to noise ratios (SNRs). Furthermore, since there is no active transmitter, the solution should be cheaper and more viable.

In a passive configuration, the receiver collects signals from third party sources, also known as illuminators of opportunity, to retrieve information from targets that have reflected the waves from those illuminators of opportunity. For this scenario, the satellites could act as illuminators. In addition, the growing number satellites, namely commercial satellite constellations, would help to provide good coverage. Besides, as the system is mounted on a CubeSat, so there is no need for atmosphere compensation proceedings. Therefore, the choice of the PBR seems appropriate.

As mentioned an advantage of using passives radars would include that the detection of the space debris would be done by recording the occultation of existing signals. Considering that everyday there are more wireless devices and users the frequency spectrum is getting accordingly crowded. Consequently, by using a passive configuration the frequency spectrum would not be as congested.

The system would be able to detect and track space objects. This information could be used to create a database of space debris that could be globally available. The database would comprise sizes, estimated orbits, trajectories and altitudes of the collected data. This information would be used to prevent space disasters and damages and to keep track on the amount of space waste the atmosphere contains.

This paper analyses and explores the possibility of using a CubeSat-mounted passive forward scattering radar (FSR) for space situational awareness purposes. More concretely, the paper examines the performance of different types of antennas that could be employed on the PBR system. This examination includes a description on how the PBR mounted on the CubeSat would work, the description of the antennas, a link budget, maximum distances and minimum detectable sizes.

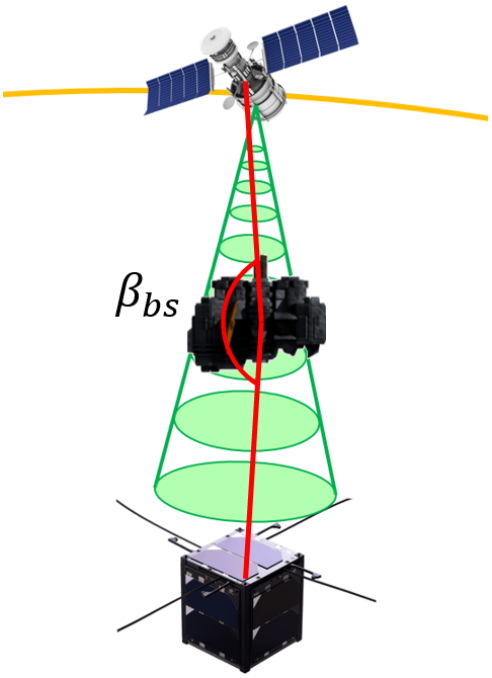

Figure 1: Satellite (transmitter) and CubeSat (receiver) configuration

2. SYSTEM DESCRIPTION

The system would be a PBR mounted on a CubeSat. The illuminator of opportunity, the transmitter, would be a satellite. The CubeSat would be placed at a lower orbit than the satellite and the possible targets would be crossing between them, figure 1. The CubeSat will be receiving the signal from the satellite with a nearly bistatic angle of: $\beta_{bs} = 180°$. This configuration is also known as forward scatter (FS) configuration. The main advantage of using the FS configuration is the enhanced radar cross section (RCS) [2] that will improve the SNR.

The maximum RCS in FS, also known as forward scatter cross section (FSCS), is:

$$\sigma_{FS} = \frac{4\pi A^2}{\lambda^2} \tag{1}$$

where A is the forward scatter area, the area of silhouette of the target, and λ is the wavelength. It can be observed that the smaller the λ the higher σ_{FS}, so an illuminator working at higher frequencies will be more desirable than one working a lower frequencies.

2.1. Illuminator of opportunity

The illuminator of opportunity ideally would be a constellation of satellites because of the large number of possible standardized illuminators of opportunity that would increase the ability of detecting space debris. For this reason, in this examination the Starlink Constellation satellites are considered as possible illuminators of opportunity.

Starlink works in the Ku-band between $10.7\,\mathrm{GHz}$ - $12.7\,\mathrm{GHz}$ [7] with channels of $250\,\mathrm{MHz}$ [3]. The effective isotropic radiated power (EIRP) is $36.71\,\mathrm{dB}$ and the satellites will be at an altitude of $550\,\mathrm{km}$ [8].

The reason for choosing Starlink is because the altitude results in a good SNR compared with other constellations, such as Iridium satellite ($780\,\mathrm{km}$) or Globalstar ($1400\,\mathrm{km}$). Another reason is the operating frequency of the satellites, which is higher compared to other satellites, in the case of Iridium the operating frequency is around $1.6\,\mathrm{GHz}$ and in the case of Globalstar the downlink is working at around $2.4\,\mathrm{GHz}$. First, as seen in equation 1, the higher the frequency, the smaller the wavelength that leads to a higher value of FSCS. Second, as is going to be seen later, in the case of dipole antennas the appropriate value is approximately $\lambda/2$, that will help the antenna to fit into the CubeSat.

2.2. Possible antennas

One of the main delimiters for weight and power consumption in the CubeSat is the antenna. The antennas are going to be tuned to $11.075\,\mathrm{GHz}$, the centre frequency of the second channel of $250\,\mathrm{MHz}$ For this analysis three different antennas are going to be observed:

- Patch antenna
- Array of patch antennas
- 3D phased array antenna

2.2.1. Patch antenna

The patch antenna will consist of a single rectangular metal patch. The advantages of using a patch antenna include low volume, size, weight, cost and processing power. Additional advantages include easier design and fabrication and a robust mounting. In the radar processing side the design will be more simple, since only one receiving structure is needed. The overall antenna will have an area of $10\times10\,\mathrm{cm}^2$, figure 2.

The maximum directivity gain for this antenna design is $14\,\mathrm{dBi}$. Figure 3 shows that there are 6 main lobes. The multiple illuminators of the constellation along with the multiple lobes will contribute to a higher probability of detecting space debris or a higher SNR. However, in the case that there were multiple pieces of space debris on the there could be a certain ambiguity with the actual position and speed direction of the targets.

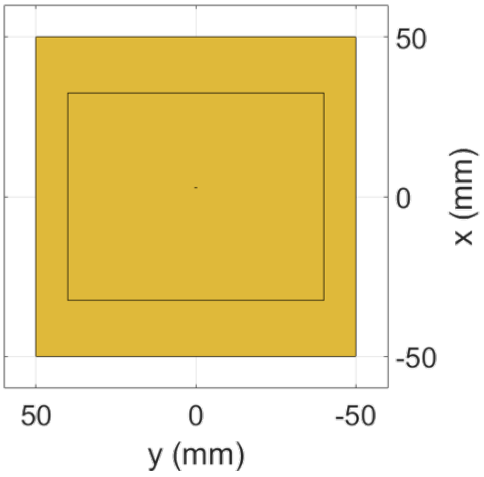

Figure 2: Single patch antenna

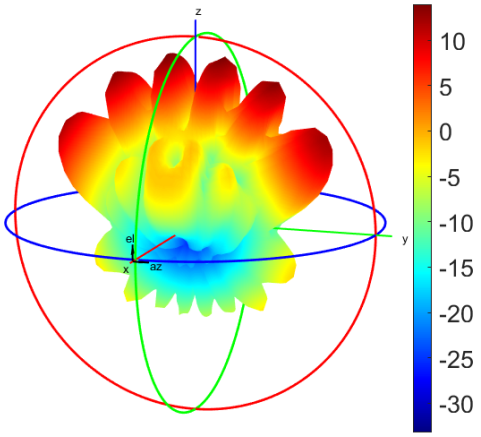

Figure 3: Directivity pattern of the patch antenna

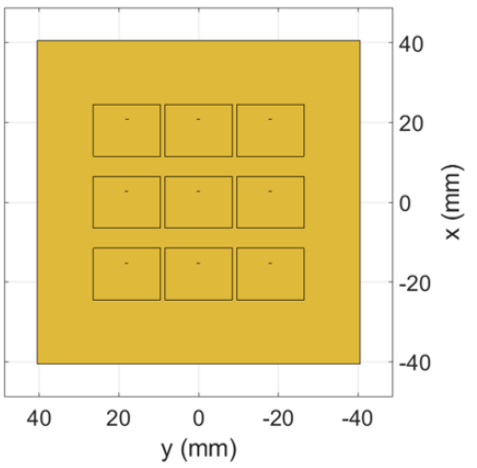

Figure 4: Array of patch antennas

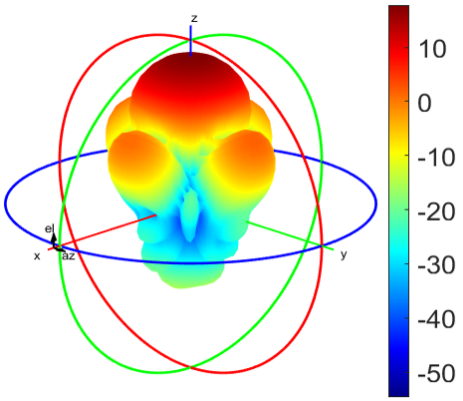

Figure 5: Directivity pattern of array of patch antennas with no phase shift

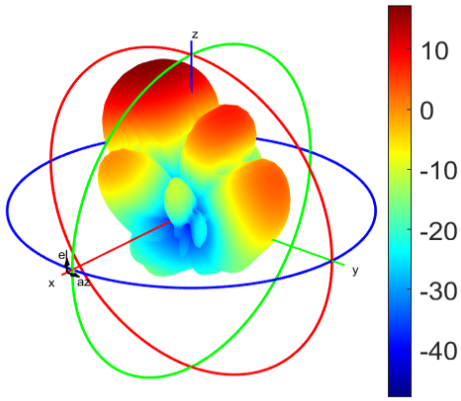

Figure 6: Directivity pattern of array of patch antennas with a phase shift of 20°

2.2.2. Array of patch antennas

The array of patch antennas will consist of 9 patch antennas arranged in a 3×3 structure, as shown in figure 4. It shares some of the advantages that the single patch antenna has, such as the lower volume, size, weight and cost. Also, as what happened with the single patch antenna, the mounting is robust and the design and manufacturing process is easier. An added advantage would be that the antenna can electrically or digitally scan the environment. Figure 4 also exhibits the area of the antenna: $8 \times 8\,\mathrm{cm}^2$.

Two different phase shifts, or beam shifts, are considered in the directivity pattern: $0°$ and $20°$. The $20°$ phase shift is due to the tracking capabilities that the system should have. The maximum directivity gain for the $0°$ shift is $17.8\,\mathrm{dBi}$, whereas for the $20°$ shift the value is $17.3\,\mathrm{dBi}$. It can be appreciated that the loss in the directivity due to the phase shift is very small, $0.5\,\mathrm{dB}$. Contrarily to the single patch antenna, as there is only one main lobe, only one beam, there would be no ambiguity if multiple targets were present in the environment.

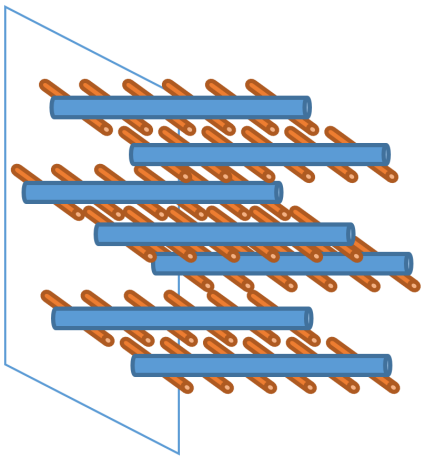

Figure 7: 3D phased array antenna

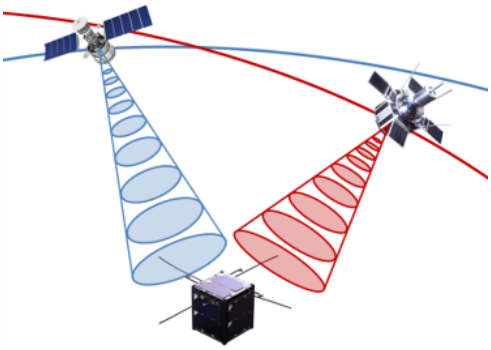

Figure 8: Digital beam forming technology

2.2.3. 3D phased array antenna (3D-PAA)

This is a novel antenna developed by Nobuyuki Kaya [4]. This antenna is composed by poles and each pole is composed by antenna dipoles with a volume of 1U, $10 \times 10 \times 10\,\mathrm{cm}^3$, and with 49 elements arranged as in figure 7. The length of the dipoles is $12.81\,\mathrm{mm}$, which is very similar to $\lambda/2 = 13.62\,\mathrm{mm}$. If the operating frequency was lower, for example if it was $2.4\,\mathrm{GHz}$, the length of the each array element would be: $\lambda/2 = 6.246\,\mathrm{cm}$ which might have prevented the antenna fitting into a volume of 1U.

Some advantages of using such antenna will be that it can electrically or digitally scan the environment. The 3D-PAA has an improved directivity compared to the other examined antennas, as it is going to be seen later. In addition, as a result of the digital beam forming technology, it could simultaneously identify signals coming from different sources, figure 8.

The maximum directivity with no phase shift is $19.5\,\mathrm{dB}$ and with a phase shift of $20°$ the directivity gain is $17.3\,\mathrm{dB}$. Unlike the case of the array of patch antennas, the loss due to the phase shift is $2.2\,\mathrm{dB}$. As seen on figures 9 and 10, the back lobes of the antenna are considerably high. In principle, this back lobes should not create

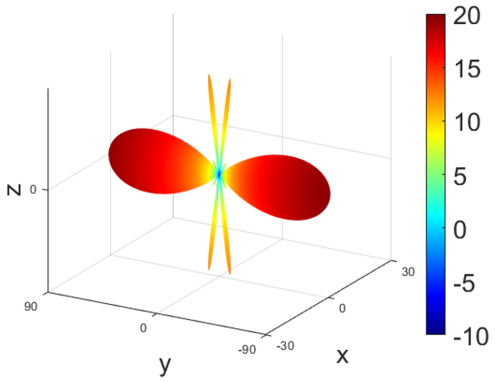

Figure 9: Directivity pattern of 3D-PAA with no phase shift

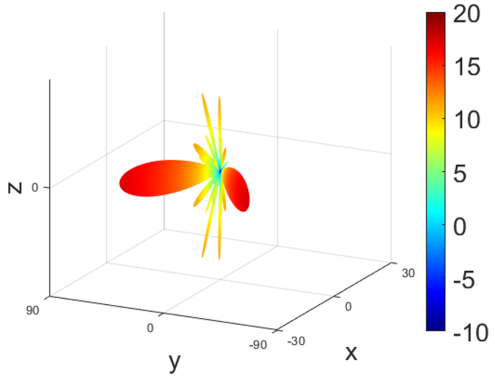

Figure 10: Directivity pattern of 3D-PAA with a phase shift of 20°

any problems since it is not expected to have any signals coming from behind. However, in order to avoid any unexpected signals, the back of the antenna could have some sort of electromagnetic absorbing material.

3. ANALYSIS

For conducting the analysis a link budget analysis is performed. The link budget is characterized by the signal-to-noise ratio (SNR) and the range radar equation (RRE):

$$SNR = \frac{EIRP\ G_r\ G_{sp}\ \lambda^2\ \sigma_{FS}}{(4\pi)^3\ R_1^2\ R_2^2\ k\ T_0\ F\ B_w\ L_s} \qquad (2)$$

where:

	Phase shift	
	0°	20°
Patch antenna	14 dBi	-
Array of patch antennas	17.8 dBi	17.3 dBi
3D-PAA	19.5 dBi	17.3 dBi

Table 1: Directivity gain for different antennas and phase shifts

- $EIRP$ is the effective isotropic radiated power
- G_r is the receiver gain. Defined as the directivity gain of the receiver antenna, $G_{r,ant}$, and the low noise amplifier (LNA) gain, G_{LNA}.
- G_{sp} is the signal processing gain. This is approximately given by the product between the transmitted pulse length and the transmitter bandwidth [1].
- λ is the wavelength
- σ_{FS} is the forward scatter cross section as defined on equation 1
- R_1 is the distance from the transmitter to the target
- R_2 is the distance from the target to the receiver
- k is the Boltzmann constant
- T_0 is the reference temperature
- F is the noise figure
- B_w is the bandwidth of the signal
- L_s are the losses

For increasing the SNR multiple transmitted pulses can be integrated, this is also known as multiple pulse integration or, simply, multiple integration [6]. Multiple integration can be done non-coherently or coherently, also known as non-coherent integration and coherent integration respectively. In non-coherent integration only the magnitude of the signal is integrated per contra in coherent integration both the in-phase and quadrature components of the signals are integrated. For the case of non-coherent integration the SNR is multiplied by a factor of $\sqrt{N}$, equation 3. Nonetheless, for the case of coherent integration the SNR is multiplied by N, equation 4. In these two cases N is the number of pulses to be integrated.

$$SNR = \frac{EIRP\ G_r\ G_{sp}\ \lambda^2\ \sigma_{FS}}{(4\pi)^3\ R_1^2\ R_2^2\ k\ T_0\ F\ B_w\ L_s} \cdot \sqrt{N} \quad (3)$$

$$SNR = \frac{EIRP\ G_r\ G_{sp}\ \lambda^2\ \sigma_{FS}}{(4\pi)^3\ R_1^2\ R_2^2\ k\ T_0\ F\ B_w\ L_s} \cdot N \quad (4)$$

3.1. Minimum detectable size

For the link analysis, for sake of simplicity, a perfect conductive sphere is assumed. The area of the silhouette of a sphere would be the area of a circle, equation 5.

$$A = \pi r^2 \quad (5)$$

Combining equations 1, 3, 4 and 5, the minimum detectable size is obtained:

$$r = 2\sqrt[4]{\frac{SNR\ R_1^2\ R_2^2\ k\ T_0\ F\ B_w\ L_s}{EIRP\ G_r\ G_{sp}\ \sqrt{N}}} \quad (6)$$

$EIRP$	36.71 dB
f_{op}	11.075 GHz
B_w	250 MHz
Gr, ant	[13.5; 17.8; 19.5]dB 17.3 dB (20°)
G_{LNA}	26 dB
N	20
CubeSat alt.	400 km
Illuminator alt.	550 km
Target alt.	400-550 km
F	10 dB
SNR	8 dB

Table 2: Minimum detectable size computing parameters

$$r = 2\sqrt[4]{\frac{SNR\ R_1^2\ R_2^2\ k\ T_0\ F\ B_w\ L_s}{EIRP\ G_r\ G_{sp}\ N}} \quad (7)$$

where r is the radius of the assumed sphere. The final parameters for calculating the minimum detectable size are shown in table 2. Similarly, the table shows that the aimed SNR is 8 dB, which as reported in [5] is enough for a good probability of detection.

According to equations 6 and 7, if either $R_1 \approx 0$ or $R_2 \approx 0$, the minimum detectable size will also be almost 0. Therefore, it is expected that when the target orbits near the transmitter or the receiver the minimum detectable size will be small. Plus, the product $R_1^2 \cdot R_2^2$ is the highest when $R_1 = R_2$. Consequently, there will be a maximum when the target is flying near the middle of the orbits of the transmitter and the receiver. Multiple integration will also factor into the minimum detectable size. $\sqrt{N}$ will be smaller than N: $\sqrt{N} \lll N$; as a result, for the same parameters, the minimum detectable size will be smaller for the non-coherent integration and larger for the coherent integration.

Regarding the influence of the antennas on the minimum detectable size, the higher the antenna gain, the smaller the minimum detectable size. Thus, the 3D-PAA, having the higher antenna gain, will have the smallest minimum detectable size, followed by the array of patch antennas and the single patch antenna. Considering all the influences and elements of the link budget, the smallest minimum detectable size will occur when coherent integration is employed with the 3D-PAA. The phase shift of 20° yields in the same directivity gain for the array of patch antennas and the 3D-PAA, so both scenarios will derive in the same minimum detectable sizes.

Figures 11, 12 and 13 show that the largest minimum detectable sizes go from 63.44 cm down to 43.62 cm, for the 3D-PAA, from 69.96 cm down to 48.11 cm, for the array of patch antennas, and from 89.61 cm down to 61.62 cm, for the patch antenna. Minimum detectable sizes are very similar and comparable when the array of patch antennas and the 3D-PAA are mounted on the CubeSat, with values of about 65 cm with integration being done non-coherently, and with values of about 45 cm with coherent integration. Using the patch antenna produces the largest minimum detectable sizes, 89.61 cm

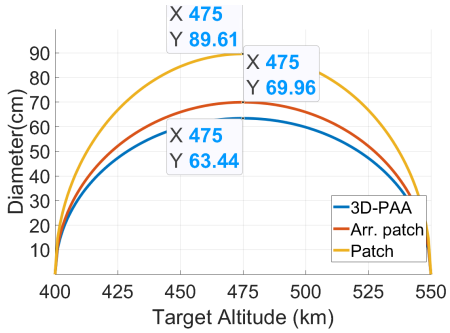

Figure 11: Minimum detectable size for different antennas with non-coherent integration

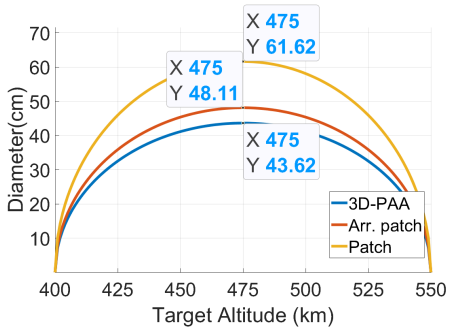

Figure 12: Minimum detectable size for different antennas with coherent integration

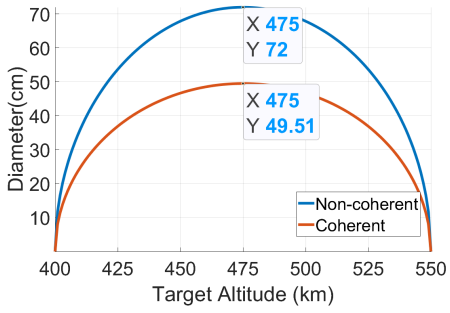

Figure 13: Minimum detectable size for non-coherent and coherent integration with a 20° phase shift

and 61.62 cm, leaving this antenna to be the inferior option.

4. CONCLUSION AND FUTURE WORK

Different types of antennas have been examined for a PBR system in a FS configuration which purpose is to detect and track space objects. Such a system could be a cheaper solution, compared to current systems. Because of the passive disposition of the radar, the frequency spectrum will not be affected, it will not contribute to the oversaturation of the spectrum.

The 3D-PAA with its almost 50 elements will consume lots of power, not only in the processing of the signals coming from each pole but also with the steering of the main beam for tracking. As a consequence of the large amount of elements, the 3D-PAA is also the biggest one in terms of volume and weight, The antenna that would have the smallest consumption, lowest cost and weight, would be the single patch antenna. A good compromise, and a better option, between both antennas is the array of patch antennas. Additionally, as seen on the minimum detectable size analysis, even though the 3D-PAA can detect smaller space debris, those detectable sizes are comparable to the ones that the array of patch antennas can identify. Besides, when the beam of the antenna is shifted both antennas will be able to detect the same sizes, so in the tracking scenario there is practically no difference between the 3D-PAA and the array of patch antennas, concluding that this last one is a better option overall.

Future work will focus on the development of the radar side of the system and the proper algorithms for the track and detection purposes. Since the 3D-PAA is too large, a way of optimizing the number of elements must be examined. The 3D-PAA could also be placed on a ground station scenario where there are no major weight and powering constraints. Plus, the multiple beam technology of the novel antenna must be studied in the track and search configuration to properly know how to exploit all its capabilities. Finally, both the antenna and the hardware will be integrated to evaluate the real system and how to coordinate the capabilities of the chosen antenna with the specifications of the hardware.

REFERENCES

1. A. R. Persico, P. Kirkland, C. Clemente, J. J. Soraghan and M. Vasile, (2019). IEEE Transactions on Aerospace and Electronic Systems, *CubeSat-Based Passive Bistatic Radar for Space Situational Awareness: A Feasibility Study*, **55**(1), 476-485.
2. Jèrome I. Glaser, (1985). IEEE Transactions on Aerospace and Electronic Systems, *Bistatic RCS of Complex Objects Near Forward Scatter*, **21**(1), 70-78.
3. Inigo del Portillo, Bruce G. Cameron and Edward F. Crawley, (2018). 69th International Astronautical

Congress (IAC), *Technical Comparison of Three Low Earth Orbit Satellite Constellation Systems to Provide Global Broadband*

4. Nobuyuki Kaya, (2018). 69th International Astronautical Congress (IAC), *New development of the phased array antenna for S-band communications*

5. James Murray, Rossina Miller, Mark Matney, and Timothy Kennedy, (2019). First International Orbital Debris Conference, *Orbital Debris Radar Measurements from the Haystack Ultra-wideband Satellite Imaging Radar (HUSIR): 2014-2017*

6. Richards, Mark A.; Scheer, James A.; Holm, William A. (ed.): *Principles of Modern Radar: Basic principles* DOI: IET Digital Library

7. *Application For Approval for Orbital Deployment and Operating Authority for the SpaceX NGSO Satellite System*, Federal Communications Commission.

8. *Application for modification of authorization for the SpaceX NGSO satellite system*, Federal Communications Commission.